Check for updates

Received: 30 June 2023 | Revised: 7 August 2023 | Accepted: 23 August 2023

DOI: 10.1002/pamm.202300158

RESEARCH ARTICLE

Numerical implementation of tension–compression asymmetry in a gradient-extended two-surface damage–plasticity model

Jian Zhang | **Tim Brepols** | **Stefanie Reese**

Institute of Applied Mechanics, RWTH Aachen University, Aachen, Germany

Correspondence
Jian Zhang, Institute of Applied Mechanics, RWTH Aachen University, Mies-van-der-Rohe-Str. 1, D-52074 Aachen, Germany.
Email: jian.zhang@ifam.rwth-aachen.de

Abstract

Based on the spectral decomposition of the strain tensor, the tension-compression asymmetry (TCA) in a gradient-extended two-surface damage-plasticity model is considered in this study. More specifically, the gradient extension is applied in the current model as a suitable damage regularization technique to prevent pathological mesh dependence issues. Furthermore, plasticity and damage are treated as distinct but strongly coupled dissipative mechanisms by using two different types of damage and yield criteria as well as the related loading/unloading conditions, respectively. Finally, a specific material parameter h_{tc} is adopted to control the degree of TCA which results in a unique damage evolution in compression.

1 | MICROMORPHIC GENERALIZATION AND WEAK FORM OF THE PROBLEM

Forest [1] generalized many existing gradient-extended models by means of the micromorphic theory. The micromorphic approach makes use of two types of variables, namely local internal variables and related additional field variables (micromorphic variable), respectively. Based on this, the present model adopts a geometrically linear, quasi-static, and purely mechanical framework, where the local damage variable D is treated as internal variable, and the micromorphic variable $\bar{D}$ is introduced by gradient effects. Moreover, the local variable D is approximately equal to the micromorphic variable $\bar{D}$ by choosing a sufficiently large coupling modulus as a penalty factor.

The linear momentum balance for the displacements $\mathbf{u}$ and the generalized force balance equation for the micromorphic variable $\bar{D}$ in the domain of body Ω are given by [2]

$$\operatorname{div}(\boldsymbol{\sigma}) + \mathbf{f} = \mathbf{0}, \qquad \operatorname{div}(\boldsymbol{b}_i) - \mathbf{a}_i = \mathbf{0}. \tag{1}$$

In the above, $\boldsymbol{\sigma}$ is the Cauchy stress tensor, $\mathbf{f}$ denotes the conventional body forces, and $\mathbf{a}_i$, $\boldsymbol{b}_i$ account for the internal forces which are related to $\bar{D}$ and its gradient $\nabla\bar{D}$, respectively. Furthermore, Dirichlet Γ_u and Neumann Γ_t parts of the boundary conditions are assumed as follows:

$$\boldsymbol{\sigma}[\mathbf{n}] = \hat{\mathbf{t}} \text{ on } \Gamma_t, \qquad \mathbf{u} = \hat{\mathbf{u}} \quad \text{on } \Gamma_u, \qquad \nabla\bar{D} \cdot \mathbf{n} = 0 \text{ on } \Gamma, \tag{2}$$

This is an open access article under the terms of the Creative Commons Attribution-NonCommercial-NoDerivs License, which permits use and distribution in any medium, provided the original work is properly cited, the use is non-commercial and no modifications or adaptations are made.
© 2023 The Authors. *Proceedings in Applied Mathematics and Mechanics* published by Wiley-VCH GmbH.

where $\mathbf{n}$ represents a unit outward normal vector at the boundary and $\hat{\mathbf{u}}$ and $\hat{\mathbf{t}}$ are prescribed displacements and tractions at the Dirichlet and Neumann boundaries, respectively. Moreover, it holds $\Gamma = \Gamma_u \cup \Gamma_t, \Gamma_u \cap \Gamma_t = \emptyset$. Finally, the weak form of the problem can be obtained from the balance equations by multiplying suitable vectorial and scalar test functions $\delta\boldsymbol{u}$ and $\delta\bar{D}$ [3]:

$$g(\mathbf{u}, \bar{D}, \delta\mathbf{u}) := \int_\Omega (\boldsymbol{\sigma} \cdot \nabla^s \delta\mathbf{u} - \mathbf{f} \cdot \delta\mathbf{u}) d\Omega - \int_{\Gamma_t} \hat{\mathbf{t}} \cdot \delta\mathbf{u} d\Gamma = 0 \quad \forall \delta\mathbf{u}, \tag{3}$$

$$h(\mathbf{u}, \bar{D}, \delta\bar{D}) := \int_\Omega -a_i\, \delta\bar{D} - \boldsymbol{b}_i \cdot \nabla\delta\bar{D}) d\Omega = 0 \quad \forall \delta\bar{D}. \tag{4}$$

2 | TENSION-COMPRESSION ASYMMETRY IN DAMAGE

The effect of tension-compression asymmetry, which is also known as the "(quasi) unilateral effect" or "microdefects/crack closure effect" [4, 5], can be observed in plenty of materials such as metals [6], ceramics [7], and geological materials [8, 9]. During the simulation of the mentioned materials, it is necessary to consider TCA to describe failure realistically by excluding spurious failure in compression. Following a common approach in the literature [5, 10], which considers TCA based on the spectral decomposition of the strain tensor, the present study extends the existing gradient-extended two-surface damageplasticity models [2, 3, 11, 12] by considering different damage evolutions in tension and compression.

2.1 | Helmholtz free energy

Prior to the consideration of TCA, the total strain is defined as $\boldsymbol{\varepsilon} := \nabla^s(\mathbf{u})$ in the present geometrically linear model, and it is assumed to be additive separable into an elastic strain $\boldsymbol{\varepsilon}_e$ and a plastic strain $\boldsymbol{\varepsilon}_p$. To model nonlinear kinematic hardening, $\boldsymbol{\varepsilon}_p$ is further split into recoverable ($\boldsymbol{\varepsilon}_{pe}$) and irrecoverable ($\boldsymbol{\varepsilon}_{pi}$) parts:

$$\boldsymbol{\varepsilon} = \boldsymbol{\varepsilon}_e + \boldsymbol{\varepsilon}_p = \boldsymbol{\varepsilon}_e + \boldsymbol{\varepsilon}_{p_e} + \boldsymbol{\varepsilon}_{p_i}. \tag{5}$$

Furthermore, the total Helmholtz free energy is defined as the state potential of the present model. It contains four parts, which are the elastic energy ψ_e, plastic energy ψ_p, damage hardening energy ψ_d, and the energy $\psi_{\bar{d}}$ related to micromorphic damage and its gradient, respectively:

$$\psi = f_{dam1}(D)\big(\psi_e(\boldsymbol{\varepsilon}_e) + \psi_p(\boldsymbol{\varepsilon}_{p_e}, \xi_p)\big) + \psi_d(\xi_d) + \psi_{\bar{d}}(D, \bar{D}, \nabla\bar{D}). \tag{6}$$

In the above, ξ_p denotes the plastic isotropic hardening variable, ξ_d is the damage hardening variable, and $f_{dam1}(D)$ is a degradation function. The internal damage variable D ranges from 0 to 1, representing material degradation in an averaged manner.

In order to describe TCA in the material behavior, an additive decomposition of the elastic part of the free energy into tension-related and compression-related parts is essential [5]. It reads

$$\psi_{\mathrm{e}}(\boldsymbol{\varepsilon}_e) = \underbrace{\left(\frac{1}{2}\lambda\left[\mathrm{tr}(\boldsymbol{\varepsilon}_e^+)\right]^2 + \mu\boldsymbol{\varepsilon}_e^+ : \boldsymbol{\varepsilon}_e^+\right)}_{\psi_{\mathrm{e}}^+} + \underbrace{\left(\frac{1}{2}\lambda[\mathrm{tr}(\boldsymbol{\varepsilon}_e^-)]^2 + \mu\boldsymbol{\varepsilon}_e^- : \boldsymbol{\varepsilon}_e^-\right)}_{\psi_{\mathrm{e}}^-}, \tag{7}$$

$$\boldsymbol{\varepsilon}_e = \boldsymbol{\varepsilon} - \boldsymbol{\varepsilon}_p = \boldsymbol{\varepsilon}_e^+ + \boldsymbol{\varepsilon}_e^-, \tag{8}$$

where λ and μ are the two Lamé constants. $\boldsymbol{\varepsilon}_e^+$ and $\boldsymbol{\varepsilon}_e^-$ denote the tension-related and the compression-related parts of the elastic strain $\boldsymbol{\varepsilon}_e$, respectively. Based on the spectral decomposition [10], the following definitions of the elastic strain parts are used:

$$\boldsymbol{\varepsilon}_e^+ = \sum_{i \in A} \varepsilon_{ei} \boldsymbol{n}_i \otimes \boldsymbol{n}_i, \quad A = \{i : \varepsilon_{ei} \geq 0\}, \tag{9}$$

$$\boldsymbol{\varepsilon}_e^- = \sum_{i \in B} \varepsilon_{ei} \boldsymbol{n}_i \otimes \boldsymbol{n}_i, \quad B = \{i : \varepsilon_{ei} < 0\}. \tag{10}$$

16177061, 2023, 2, Downloaded from https://onlinelibrary.wiley.com/doi/10.1002/pamm.202300158 by Rwth Aachen Hochschulbibliothek, Wiley Online Library on [25/04/2024]. See the Terms and Conditions (https://onlinelibrary.wiley.com/terms-and-conditions) on Wiley Online Library for rules of use; OA articles are governed by the applicable Creative Commons License

Here, ε_{ei} and $\boldsymbol{n}_i$ are the eigenvalues and the eigenvectors of the elastic strain $\boldsymbol{\varepsilon}_e$, respectively. With this at hand, the total energy can be rewritten as

$$\psi = f_{dam1}(D)\left(\psi_e^+(\boldsymbol{\varepsilon}_e^+) + \psi_p(\boldsymbol{\varepsilon}_{p_e}, \xi_p)\right) + f_{dam2}(D)\psi_e^-(\boldsymbol{\varepsilon}_e^-) + \psi_d(\xi_d) + \psi_{\bar{d}}(D, \bar{D}, \nabla\bar{D}), \tag{11}$$

$$f_{dam1}(D) = (1-D)^2, \qquad f_{dam2}(D) = (1-h_{tc}D)^2. \tag{12}$$

There are two degradation functions involved. $\psi_e^+(\boldsymbol{\varepsilon}_e^+)$ and $\psi_e^-(\boldsymbol{\varepsilon}_e^-)$ are degraded by $f_{dam1}(D)$ and $f_{dam2}(D)$, respectively. Furthermore, by referring to the work of Miehe et al [13], $\psi_p(\boldsymbol{\varepsilon}_{p_e})$ is degraded by $f_{dam1}(D)$, which means that plasticity in compression still drives damage evolution as in tension. However, further improvements of TCA in plasticity modeling should be considered in the future. The parameter h_{tc} in the second degradation function, which ranges from 0 to 1, controls the degree of TCA. The degree of TCA increases if h_{tc} gets smaller.

The details of the remaining parts in the Helmholtz free energy ψ are as follows:

$$\psi_p = \frac{a}{2}\boldsymbol{\varepsilon}_{p_e}\cdot\boldsymbol{\varepsilon}_{p_e} + e\left(\xi_p + \frac{\exp(-f\,\xi_p)-1}{f}\right), \tag{13}$$

$$\psi_d = r\left(\xi_d + \frac{\exp(-s\,\xi_d)-1}{s}\right), \tag{14}$$

$$\psi_{\bar{d}} = \frac{1}{2}H(D-\bar{D})^2 + \frac{1}{2}A\nabla\bar{D}\cdot\nabla\bar{D} \tag{15}$$

The plastic energy ψ_p comprises two terms: the first one pertains to nonlinear kinematic hardening, while the second term relates to nonlinear isotropic hardening. a, e, and f are constant material parameters about material properties. Moreover, the energy contribution ψ_d comes from nonlinear damage hardening in a form analogous to isotropic hardening in plasticity, with r and s being two material parameters. Finally, the micromorphic damage part of the energy $\psi_{\bar{d}}$ contains two terms. The first term serves as an energetic penalty for the discrepancy between the local damage variable and the micromorphic damage variable. The second term, associated with the gradient of the micromorphic damage variable, characterizes the influence exerted by the gradient. The parameter H is provided as a penalty factor, whereas parameter A implicitly introduces an internal length scale into the formulation.

2.2 | State relations and thermodynamic conjugate forces

The mechanical energy stored within a body during a deformation process is constrained by the second law of thermodynamics, ensuring that it does not surpass the mechanical work generated on the body. It implies that the total mechanical dissipation within the body should consistently maintain a positive value. The isothermal local form of the Clausius–Duhem inequality is used to derive consistent state relations of the model and reads

$$-\dot{\psi} + \boldsymbol{\sigma}\cdot\dot{\boldsymbol{\varepsilon}} + \underbrace{a_{\mathrm{i}}\dot{\bar{D}} + \mathbf{b}_{\mathrm{i}}\cdot\nabla\dot{\bar{D}}}_{\text{Micromorphic extension}} \geq 0. \tag{16}$$

The above inequality includes the additional micromorphic extension terms that capture the influences of both the micromorphic damage and its first gradient in the second law of thermodynamics. Furthermore, the inequality can be rewritten by substituting the Helmholtz free energy in Equation (16) (see [5]):

$$\begin{aligned}&\left(\boldsymbol{\sigma}^+ - \frac{\partial\psi}{\partial\boldsymbol{\varepsilon}_e^+} : \frac{\partial\boldsymbol{\varepsilon}_e^+}{\partial\boldsymbol{\varepsilon}_e}\right)\cdot\dot{\boldsymbol{\varepsilon}} + \left(\boldsymbol{\sigma}^- - \frac{\partial\psi}{\partial\boldsymbol{\varepsilon}_e^-} : \frac{\partial\boldsymbol{\varepsilon}_e^-}{\partial\boldsymbol{\varepsilon}_e}\right)\cdot\dot{\boldsymbol{\varepsilon}} + \left(a - \frac{\partial\psi}{\partial\bar{D}}\right)\dot{\bar{D}}\\ &+ \left(\boldsymbol{b} - \frac{\partial\psi}{\partial\nabla\bar{D}}\right)\cdot\nabla\dot{\bar{D}} + \frac{\partial\psi}{\partial\boldsymbol{\varepsilon}_e}\cdot\dot{\boldsymbol{\varepsilon}}_p - \frac{\partial\psi}{\partial\boldsymbol{\varepsilon}_{p_e}}\cdot\dot{\boldsymbol{\varepsilon}}_{p_e} - \frac{\partial\psi}{\partial\xi_p}\cdot\dot{\xi}_p - \frac{\partial\psi}{\partial D}\cdot\dot{D} - \frac{\partial\psi}{\partial\xi_d}\cdot\dot{\xi}_d \geq 0\end{aligned} \tag{17}$$

To better describe the influence of different degradation functions if when TCA is considered, the elastic strain-related terms in the inequality are divided into two parts, which are the tension-related and compression-related parts,

16177061, 2023, 2, Downloaded from https://onlinelibrary.wiley.com/doi/10.1002/pamm.202300158 by Rwth Aachen Hochschulbibliothek, Wiley Online Library on [25/04/2024]. See the Terms and Conditions (https://onlinelibrary.wiley.com/terms-and-conditions) on Wiley Online Library for rules of use; OA articles are governed by the applicable Creative Commons License

respectively. As shown, $\boldsymbol{\sigma}^+$ denotes the tension-related Cauchy stress which is effected by f_{dam1}, while $\boldsymbol{\sigma}^-$ is the compression-related Cauchy stress which is effected by f_{dam2}. The state relations of the model are obtained by deliberately setting the expressions in parentheses to zero. This leads to

$$\boldsymbol{\sigma} = \boldsymbol{\sigma}^+ + \boldsymbol{\sigma}^-, \tag{18}$$

$$\boldsymbol{\sigma}^+ = \frac{\partial \psi}{\partial \boldsymbol{\varepsilon}_e^+} : \frac{\partial \boldsymbol{\varepsilon}_e^+}{\partial \boldsymbol{\varepsilon}_e}, \qquad \boldsymbol{\sigma}^- = \frac{\partial \psi}{\partial \boldsymbol{\varepsilon}_e^-} : \frac{\partial \boldsymbol{\varepsilon}_e^-}{\partial \boldsymbol{\varepsilon}_e}, \tag{19}$$

$$a_i = \frac{\partial \psi}{\partial \bar{D}} = -H(D - \bar{D}), \qquad \boldsymbol{b}_i = \frac{\partial \psi}{\partial \nabla \bar{D}} = A\,\nabla \bar{D}. \tag{20}$$

The total Cauchy stress $\boldsymbol{\sigma}$ is equal to the sum of $\boldsymbol{\sigma}^+$ and $\boldsymbol{\sigma}^-$. Moreover, the internal forces a_i and $\boldsymbol{b}_i$ are obtained based on the further state relations related to the micromorphic extension. The remaining portion on the left side should remain greater than or equal to zero to ensure the validity of the dissipation inequality. Additionally, certain abbreviations have been introduced to facilitate the notation of the thermodynamic conjugate forces in the model, leading to

$$\boldsymbol{\sigma} \cdot \dot{\boldsymbol{\varepsilon}}_p - \underbrace{\frac{\partial \psi}{\partial D}}_{:=Y} \dot{D} - \underbrace{\frac{\partial \psi}{\partial \boldsymbol{\varepsilon}_{p_e}}}_{:=\boldsymbol{\chi}_p} \cdot \dot{\boldsymbol{\varepsilon}}_{p_e} - \underbrace{\frac{\partial \psi}{\partial \xi_p}}_{:=q_p} \dot{\xi}_p - \underbrace{\frac{\partial \psi}{\partial \xi_d}}_{:=q_d} \dot{\xi}_d \geq 0, \tag{21}$$

$$\boldsymbol{\chi} := \frac{\partial \psi}{\partial \boldsymbol{\varepsilon}_{p_e}} = f_{dam1}\, a\, \boldsymbol{\varepsilon}_{p_e}, \tag{22}$$

$$q_p := \frac{\partial \psi}{\partial \xi_p} = f_{dam1}\, e\big(1 - \exp(-f\, \xi_p)\big), \tag{23}$$

$$q_d := \frac{\partial \psi}{\partial \xi_d} = r(1 - \exp(-s\, \xi_d)), \tag{24}$$

$$Y := -\frac{\partial \psi}{\partial D} = 2(1 - D)\big(\psi_e^+ + \psi_p\big) + 2(1 - h_{tc}\, D)\psi_e^- - H(D - \bar{D}). \tag{25}$$

In the above, $\boldsymbol{\chi}$ is the plastic back stress related to nonlinear kinematic hardening. q_p denotes the thermodynamic conjugate force related to isotropic hardening. q_d represents the stress induced by damage hardening. Furthermore, Y is the damage conjugate force which includes tension-related and compression-related elastic energy, as well as plastic contributions. Besides, there is an influence of the micromorphic damage variable $\bar{D}$ in the expression of Y, such that the constitutive equations obtain a nonlocal character.

2.3 | Two-surface damage–plasticity formulation

In the current model, a "two-surface" strategy is employed, whereby the yield function, damage function, and their respective loading/unloading conditions are treated as distinct entities. As a result, damage and plasticity are regarded as independent yet coupled physical mechanisms.

2.3.1 | Plasticity modeling

In this study, a standard deviatoric von Mises-type yield function expressed in terms of effective variables is taken into account. The expression of the yield function reads

$$\Phi_p(\tilde{\boldsymbol{\sigma}}, \tilde{\boldsymbol{\chi}}, \tilde{q}_p) = \sqrt{\frac{3}{2}}\, \|\tilde{\boldsymbol{\sigma}}' - \tilde{\boldsymbol{\chi}}'\| - \big(\sigma_0 + \tilde{q}_p\big) \;\leq\; 0. \tag{26}$$

16177061, 2023, 2, Downloaded from https://onlinelibrary.wiley.com/doi/10.1002/pamm.202300158 by Rwth Aachen Hochschulbibliothek, Wiley Online Library on [25/04/2024]. See the Terms and Conditions (https://onlinelibrary.wiley.com/terms-and-conditions) on Wiley Online Library for rules of use; OA articles are governed by the applicable Creative Commons License

Here, σ_0 denotes the initial yield stress, whereas $\tilde{\boldsymbol{\sigma}}'$ and $\tilde{\boldsymbol{\chi}}'$ are the effective deviatoric Cauchy stress and back stress, respectively. Since TCA in damage is considered in the current study, the effective stress-like quantities differ from their conventional definitions, that is,

$$\tilde{\boldsymbol{\chi}} := \frac{\boldsymbol{\chi}}{f_{\text{dam1}}(D)}, \qquad \tilde{q}_p := \frac{q_p}{f_{\text{dam1}}(D)}, \tag{27}$$

$$\tilde{\boldsymbol{\sigma}} := \frac{\boldsymbol{\sigma}^+}{f_{\text{dam1}}(D)} + \frac{\boldsymbol{\sigma}^-}{f_{\text{dam2}}(D)}. \tag{28}$$

Furthermore, the following thermodynamically consistent plastic evolution equations for the strain-like plastic internal variables are postulated:

$$\dot{\boldsymbol{\varepsilon}}_p = \dot{\lambda}_p \frac{\partial \Phi_p}{\partial \boldsymbol{\sigma}} = \sqrt{\frac{3}{2}} \frac{\dot{\lambda}_p}{f_{dam1}} \frac{\boldsymbol{\sigma}' - \boldsymbol{\chi}'}{\| \boldsymbol{\sigma}' - \boldsymbol{\chi}' \|}, \tag{29}$$

$$\dot{\boldsymbol{\varepsilon}}_{p_i} = \frac{\dot{\lambda}_p}{f_{dam1}} \frac{b}{a} \tilde{\boldsymbol{\chi}}' = \frac{\dot{\lambda}_p}{f_{dam1}} b\, \boldsymbol{\varepsilon}_{p_e}, \tag{30}$$

$$\dot{\xi}_p = -\dot{\lambda}_p \frac{\partial \Phi_p}{\partial q_p} = \frac{\dot{\lambda}_p}{f_{dam1}}. \tag{31}$$

In the above, b is an additional material constant related to nonlinear kinematic hardening and $\dot{\lambda}_p$ denotes the plastic multiplier. Finally, the loading/unloading conditions for plasticity listed below need to be satisfied during the simulation:

$$\dot{\lambda}_p \geq 0, \quad \Phi_p \leq 0, \quad \dot{\lambda}_p \Phi_p = 0. \tag{32}$$

2.3.2 | Damage modeling

The damage loading function is defined as [3]:

$$\Phi_d(Y, q_d) = Y - (Y_0 + q_d) \ \leq \ 0, \tag{33}$$

where Y_0 denotes the initial damage threshold. Φ_d is chosen as an associative flow potential to derive evolution equations of the strain-like damage variables, which are defined as

$$\dot{D} = \dot{\lambda}_d \frac{\partial \Phi_d}{\partial Y}, \qquad \dot{\xi}_d = -\dot{\lambda}_d \frac{\partial \Phi_d}{\partial q_d}, \tag{34}$$

Here $\dot{\lambda}_d$ denotes the damage multiplier. In analogy to plasticity, the following loading/unloading conditions for damage need to be fulfilled as well:

$$\dot{\lambda}_d \geq 0, \quad \Phi_d \leq 0, \quad \dot{\lambda}_d \Phi_d = 0. \tag{35}$$

3 | NUMERICAL EXAMPLES

3.1 | Studies at the integration point level

A single three-dimensional finite element model with unit length is used to investigate the effect of TCA, where the standard three-dimensional eight-node brick element with full integration is adopted. Moreover, the performances of different values of h_{tc} are compared under uniaxial and shear loading, respectively. The loading and boundary conditions are shown in Figure 1; states of uniaxial and shear loading are realized by a horizontal force $F(t)$, respectively. Finally, the used material parameters are prescribed as $\lambda = 5000$ MPa , $\mu = 7500$ MPa , $\sigma_0 = 20$ MPa , $a = 1900$ MPa , $b = 8.5, e = 400$ MPa , $f = 2.5, Y_0 = 0.1$ MPa , $r = 1$ MPa , $s = 1, H = 10^5$ MPa , $A = 10$ MPa mm^2.

16177061, 2023, 2, Downloaded from https://onlinelibrary.wiley.com/doi/10.1002/pamm.202300158 by Rwth Aachen Hochschulbibliothek, Wiley Online Library on [25/04/2024]. See the Terms and Conditions (https://onlinelibrary.wiley.com/terms-and-conditions) on Wiley Online Library for rules of use; OA articles are governed by the applicable Creative Commons License

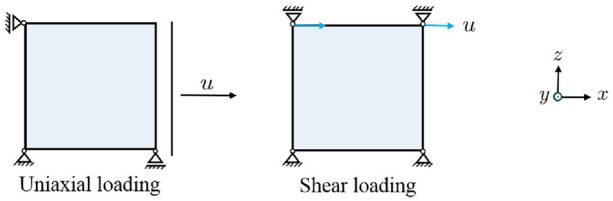


FIGURE 1 Loading and boundary conditions.

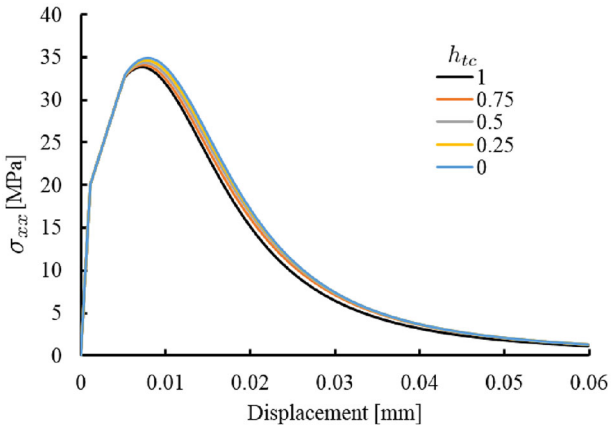


FIGURE 2 Load–displacement curves under uniaxial tension.

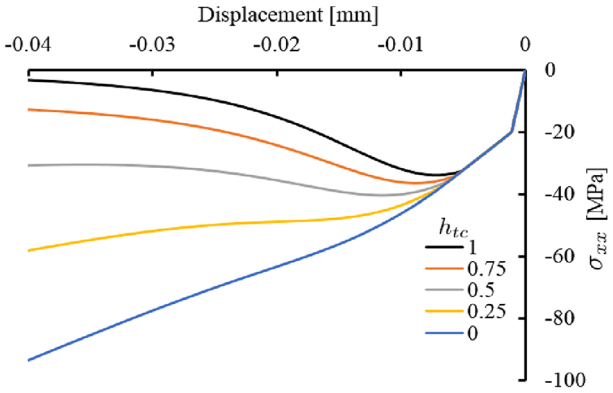


FIGURE 3 Load–displacement curves under uniaxial compression.

The degree of TCA increases if h_{tc} gets smaller. The load–displacement curves under uniaxial tension are shown in Figure 2. The simulation results show that, as the degree of TCA increases, the stress σ_{xx} at damage initiation will show a minor increase, which indicates that the effect of TCA on uniaxial tensile loading is quite small. However, the load–displacement curves in Figures 3 and 4 show that TCA has a significant influence on the simulation under uniaxial compression and shear loading. The effects are mainly manifested in two aspects. First, as the degree of TCA increases, the absolute value of the stress σ_{xx} (for uniaxial compression) or σ_{xz} (for shear loading) at damage onset increases significantly. Second, if h_{tc} is equal to 1, the damage variable D increases rapidly after the damage threshold is reached, and the absolute value of the stress σ_{xx} (uniaxial compression) or σ_{xz} (shear loading) decreases significantly because the damage-induced softening effect is greater than the plastic hardening effect. However, after applying TCA to counteract the spurious damage in compression, the damage-induced stress softening is diminished, and the absolute value of σ_{xx} (for uniaxial compression) or σ_{xz} (for shear loading) first decreases and then gradually increases after the damage threshold is reached, and the absolute value of the stress keeps increasing when h_{tc} is 0. Besides, the effect of TCA in the current two-surface damage–plasticity model is comparable to the results of brittle damage in the literature [5]. Finally,

16177061, 2023, 2, Downloaded from https://onlinelibrary.wiley.com/doi/10.1002/pamm.202300158 by Rwth Aachen Hochschulbibliothek, Wiley Online Library on [25/04/2024]. See the Terms and Conditions (https://onlinelibrary.wiley.com/terms-and-conditions) on Wiley Online Library for rules of use; OA articles are governed by the applicable Creative Commons License

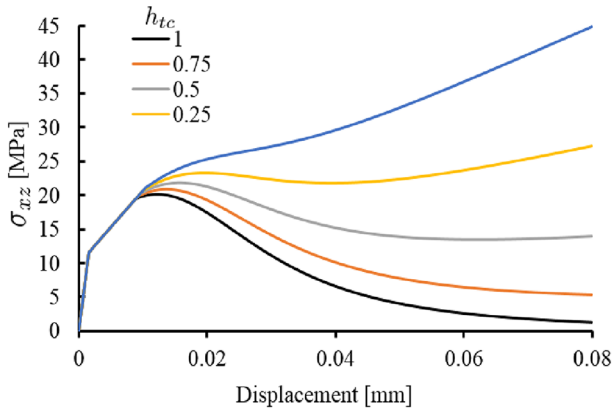


FIGURE 4 Load–displacement curves under shear loading.

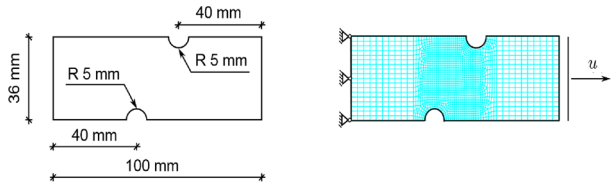


FIGURE 5 Geometry, dimensions, and boundary conditions of the asymmetrically notched specimen.

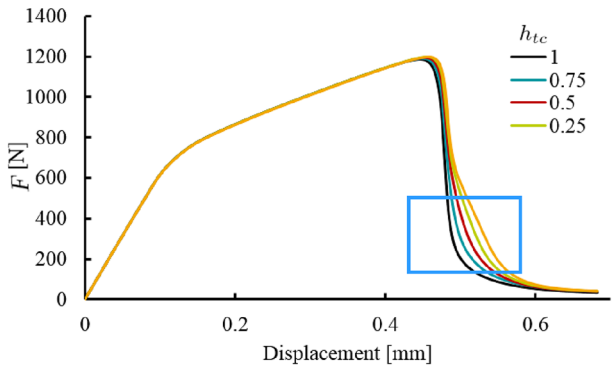


FIGURE 6 Force–displacement curves for different values of h_{tc}.

it is worth to mention that the relationship between plastic hardening and damage evolution in compression should be further investigated in future work.

3.2 | Structural example

The second numerical example is a two-dimensional plane strain specimen with asymmetric notches, where the standard two-dimensional four-node quadrilateral element with full integration is employed. As shown in Figure 5, a sample with a length of 100 mm and a width of 36 mm has a 5-mm diameter notch at the top and bottom, respectively. Furthermore, the boundary conditions for a state of uniaxial tension are given in Figure 5, where the left edge of the specimen is fully fixed while a horizontal force F is applied at its right edge.

The simulation results are obtained by using a converged mesh distribution with 1624 elements. Figure 6 presents the force–displacement curves considering TCA, and Y_0 is 0.3 MPa. Analogous to the simulation results at the integration point, the maximum force at damage onset has a minor increase with the decrease of h_{tc}. In addition, the curves within the rectangular region significantly differ for different h_{tc}, which can be attributed to the effect of TCA counteracting

16177061, 2023, 2, Downloaded from https://onlinelibrary.wiley.com/doi/10.1002/pamm.202300158 by Rwth Aachen Hochschulbibliothek, Wiley Online Library on [25/04/2024]. See the Terms and Conditions (https://onlinelibrary.wiley.com/terms-and-conditions) on Wiley Online Library for rules of use; OA articles are governed by the applicable Creative Commons License

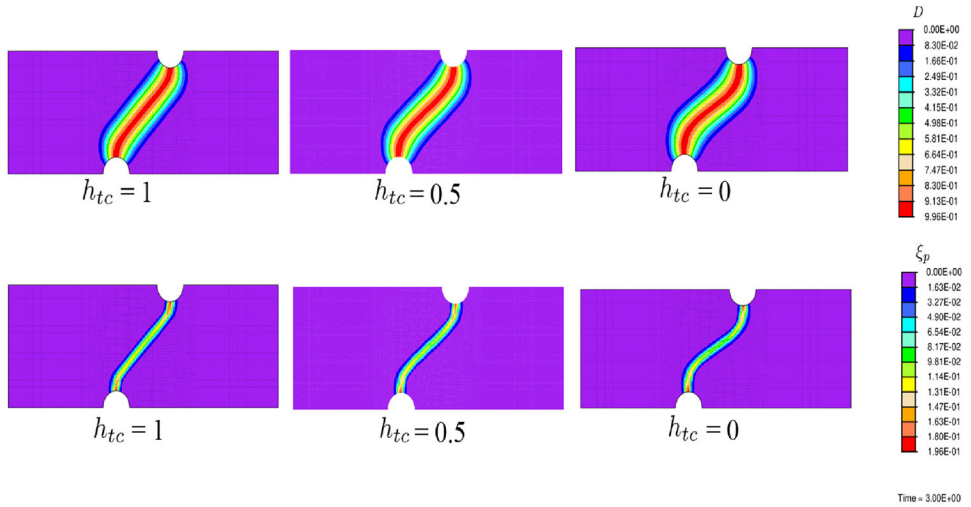


FIGURE 7 Damage contours D (top) and accumulated plastic strain ξ_p (bottom) for different values of h_{tc}.

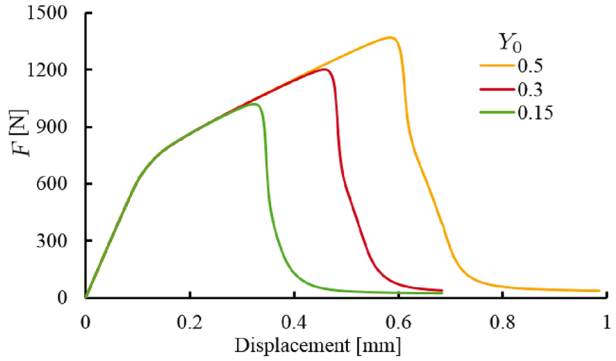


FIGURE 8 Force–displacement curves for different values of Y_0.

spurious damage in compression. As shown by the contours of D and ξ_p in Figure 7, damage propagates in the interior of the asymmetric sample and eventually forms a "crack," which connects the two notches. The fully developed failure zone has a slight S-like shape, and the influence of TCA can be measured by the curvature of the failure zone, which increases with the decrease of h_{tc}. The curvature is maximum if h_{tc} equals 0, as there is no evolution of damage in compression.

In Figure 8, the influence of the damage threshold Y_0 is demonstrated, and the value of h_{tc} is set to 0. As expected, a higher Y_0 value postpones the onset of damage. Besides, the effect of TCA becomes more apparent as the damage threshold increases, which can be more clearly observed in combination with the contours of D and ξ_p in Figure 9. The curvature of the "S" shaped failure zone formed between the two notches increases with the increase of Y_0.

4 | CONCLUSION

The numerical implementation of TCA in a gradient-extended two-surface damage–plasticity model has been presented in this work. More precisely, based on the spectral decomposition of the elastic strain tensor, the elastic energy is split into tension-related and compression-related parts. By multiplying two different degradation functions, different damage evolutions in tension and compression are obtained. Subsequently, the effects of TCA at the integration points and in a representative structural specimen are investigated through several numerical examples. The results show that the maximum force at the onset of damage increases if TCA is taken into account. Besides, in the selected asymmetrically notched specimen, the shape of the fully developed failure zone is influenced by TCA as well, where the curvature of the failure zone increases for decreasing of h_{tc}. In future studies, it is essential to further investigate the relationship between plastic

16177061, 2023, 2, Downloaded from https://onlinelibrary.wiley.com/doi/10.1002/pamm.202300158 by Rwth Aachen Hochschulbibliothek, Wiley Online Library on [25/04/2024]. See the Terms and Conditions (https://onlinelibrary.wiley.com/terms-and-conditions) on Wiley Online Library for rules of use; OA articles are governed by the applicable Creative Commons License

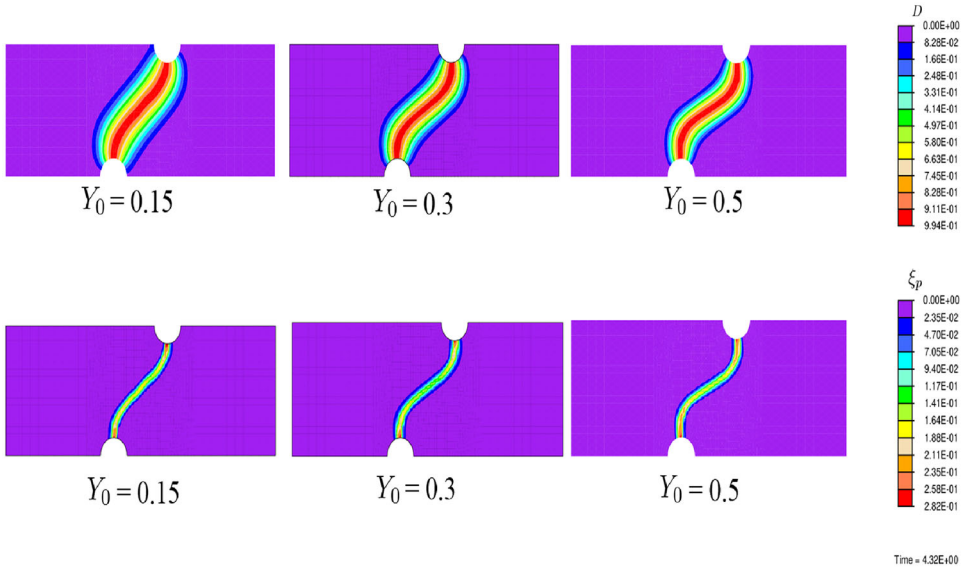


FIGURE 9 Damage contours D (top) and accumulated plastic strain ξ_p (bottom) for different values of Y_0.

hardening and the damage evolution to improve the performance of the present model in counteracting spurious damage in compression.

ACKNOWLEDGMENTS

Financial support from the China Scholarship Council is gratefully acknowledged. Furthermore, S. Reese and T. Brepols thankfully acknowledge the funding of the project RE 1057/51-1 (project number 453715964) by the German Research Foundation (DFG).

Open access funding enabled and organized by Projekt DEAL.

ORCID

Jian Zhang https://orcid.org/0000-0002-0431-0191
Tim Brepols https://orcid.org/0000-0002-1039-1776

REFERENCES

1. Forest, S. (2009). Micromorphic approach for gradient elasticity, viscoplasticity, and damage. *Journal of Engineering Mechanics*, *135*(3), 117–131.
2. Brepols, T., Wulfinghoff, S., & Reese, S. (2017). Gradient-extended two-surface damage-plasticity: Micromorphic formulation and numerical aspects. *International Journal of Plasticity*, *97*, 64–106.
3. Brepols, T., Wulfinghoff, S., & Reese, S. (2018). A Micromorphic Damage-Plasticity Model to Counteract Mesh Dependence in Finite Element Simulations Involving Material Softening. In J. Soric, P. Wriggers, & O. Allix (Eds.). *Multiscale modeling of heterogeneous structures* (pp. 235–255). Springer.
4. Murakami, S. (1988). Mechanical modeling of material damage. *Journal of Applied Mechanics*, *55*(2), 280–286.
5. Fassin, M., Eggersmann, R., Wulfinghoff, S., & Reese, S. (2019). Efficient algorithmic incorporation of tension compression asymmetry into an anisotropic damage model. *Computer Methods in Applied Mechanics and Engineering*, *354*, 932–962.
6. Wei, Z., Zistl, M., & Gerke, S., et al. (2022). Analysis of ductile damage and fracture under reverse loading. *International Journal of Mechanical Sciences*, *228*, 107476.
7. Chaboche, J., Lesne, P., & Maire, J. (1995). Continuum damage mechanics, anisotropy and damage deactivation for brittle materials like concrete and ceramic composites. *International Journal of Damage Mechanics*, *4*(1), 5–22.
8. Mazars, J., Berthaud, Y., & Ramtani, S. (1990). The unilateral behaviour of damaged concrete. *Engineering Fracture Mechanics*, *35*(4-5), 629–635.
9. Berthaud, Y., La Borderie, C., & Ramtani, S. (1990). Damage modeling and crack closure effect. *Damage Mech. Engrg. Mater. ASME AMD*, *109*, 263–276.
10. Miehe, C., Hofacker, M., & Welschinger, F. (2010). A phase field model for rate-independent crack propagation: Robust algorithmic implementation based on operator splits. *Journal of Engineering Mechanics*, *199*(45-48), 2765–2778.

16177061, 2023, 2, Downloaded from https://onlinelibrary.wiley.com/doi/10.1002/pamm.202300158 by Rwth Aachen Hochschulbibliothek, Wiley Online Library on [25/04/2024]. See the Terms and Conditions (https://onlinelibrary.wiley.com/terms-and-conditions) on Wiley Online Library for rules of use; OA articles are governed by the applicable Creative Commons License

11. Zhang, J., Brepols, T., & Reese, S. (2023). A two-surface damage-plasticity model based on a DruckerPrager yield criterion. *Proceedings in Applied Mathematics and Mechanics*, *22*(1), e202200296.
12. Harandi, A., Tabib, M., Alatassi, B., Brepols, T., Rezaei, S., & Reese, S. (2023). A comparative study between phase-field and micromorphic gradient-extended damage models for brittle fracture. *Proceedings in Applied Mathematics and Mechanics*, *22*(1), e202000110.
13. Miehe, C., Aldakheel, F., & Raina, A. (2016). Phase field modeling of ductile fracture at finite strains: A variational gradient-extended plasticity-damage theory. *International Journal of Plasticity*, *84*, 1–32.

How to cite this article: Zhang, J., Brepols, T., & Reese, S. (2023). Numerical implementation of tension–compression asymmetry in a gradient-extended two-surface damage–plasticity model. *Proceedings in Applied Mathematics and Mechanics*, *23,* e202300158. https://doi.org/10.1002/pamm.202300158

16177061, 2023, 2, Downloaded from https://onlinelibrary.wiley.com/doi/10.1002/pamm.202300158 by Rwth Aachen Hochschulbibliothek, Wiley Online Library on [25/04/2024]. See the Terms and Conditions (https://onlinelibrary.wiley.com/terms-and-conditions) on Wiley Online Library for rules of use; OA articles are governed by the applicable Creative Commons License